Influence of an Intermolecular Charge-Transfer State on Excited-State Relaxation Dynamics: Solvent Effect on the Methylnaphthalene−Oxygen System and its Significance for Singlet Oxygen Production

Poul-Gudmund Jensen, Jacob Arnbjerg, Lars Poulsen Tolbod, Rasmus Toftegaard, and Peter R. Ogilby*

Center for Oxygen Microscopy and Imaging, Department of Chemistry, Aarhus University, DK-8000 Århus, Denmark

Received: June 18, 2009; Revised Manuscript Received: July 24, 2009

The extent to which an intermolecular charge-transfer (CT) state can influence excited-state relaxation dynamics is examined for the system wherein 1-methylnaphthalene (MN) interacts with molecular oxygen. The MN-O_2 system is ideally suited for such a study because excited states can be independently accessed by (i) irradiation into the discrete MN-O_2 CT absorption band, (ii) direct irradiation of MN, and (iii) the photosensitized production of triplet state MN. Changing the solvent in which the MN-O_2 system is dissolved influences the MN-dependent photoinduced production of singlet oxygen, $O_2(a^1\Delta_g)$, which, in turn, yields information about fundamental concepts of state mixing. Results of experiments conducted in the polar solvent acetonitrile differ substantially from those obtained from the nonpolar solvent cyclohexane. The data reflect differences in the energy and behavior of the solvent-equilibrated MN-O_2 CT state, CT_{SE}, and the extent to which this state couples to other states of the MN-O_2 system. In particular, the data are consistent with a model where both the MN triplet state and the MN-O_2 CT_{SE} state are immediate precursors of $O_2(a^1\Delta_g)$. Although the work reported herein is of direct and practical significance for the wide variety of systems in which $O_2(a^1\Delta_g)$ can be produced upon irradiation, it also serves as an accessible model for a study of general issues pertinent to state mixing and the solvent-dependent dynamics of CT-mediated excited-state relaxation.

Introduction

It has long been known that a unique absorption band can appear when an organic molecule, M, is exposed to ground-state molecular oxygen, $O_2(X^3\Sigma_g^-)$. Although oxygen-dependent spectra of organic molecules were extensively studied in the 1950s by Evans,[1,2] among others, it was a seminal paper in 1960 by Tsubomura and Mulliken[3] that put key aspects of this issue into the correct perspective. In this latter work, it was proposed that these unique oxygen-dependent bands arise as a consequence of light absorption by an ephemeral ground-state collision complex between M and $O_2(X^3\Sigma_g^-)$ to populate a charge-transfer (CT) state, $[M^{\bullet+}\cdots O_2^{\bullet-}]$. Although this CT state is generally represented as a radical ion pair, complete electron transfer from M to O_2 does not necessarily occur.

As the study of photosensitized oxygenation reactions rapidly evolved through the 1960s and later, it became clear that this M-O_2 CT state could play a significant role in the collision-dependent deactivation of (i) an excited electronic state of M by $O_2(X^3\Sigma_g^-)$, including deactivation that resulted in energy transfer to produce singlet oxygen, $O_2(a^1\Delta_g)$,[4−10] and of (ii) $O_2(a^1\Delta_g)$ by ground-state M.[11−13] These processes were often conveniently discussed in terms of transitions between various states of the M-O_2 complex (the so-called oxciplex[14,15]) wherein M perturbed the isolated O_2 molecule and, vice versa, where O_2 perturbed isolated M (Figure 1).[16] Moreover, it was clearly recognized that it was not necessary to directly populate the M-O_2 CT state to realize its effects. With this model in mind, as illustrated in Figure 1 for a comparatively high-energy CT state, it is seen that one must consider mechanisms by which various states of the M-O_2 complex can mix.[4,16−18]

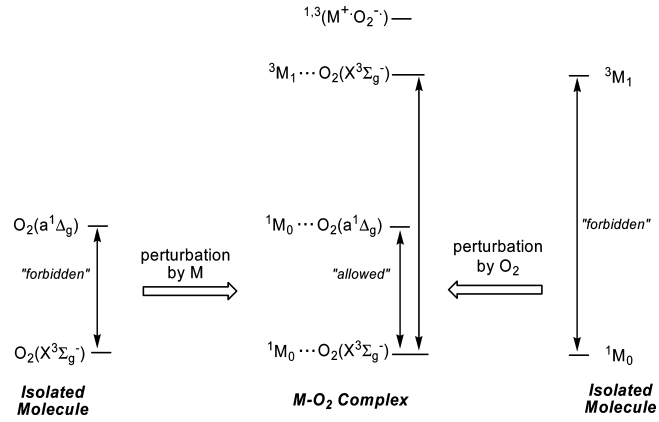

Figure 1. Diagram illustrating selected states of the M-O_2 complex. By virtue of orbital overlap and the creation of discrete new wave functions, transitions formally forbidden in the isolated molecules can become allowed in the complex.

With respect to the $O_2(X^3\Sigma_g^-)$-induced deactivation of an excited state of M and the energy transfer process that results in $O_2(a^1\Delta_g)$ production, there is now ample evidence to indicate that an increase in the amount of CT character, both within a given M (intramolecular CT) and in the M-O_2 encounter complex (intermolecular CT), adversely affects the yield of $O_2(a^1\Delta_g)$.[9,19−21] For the intramolecular case, the CT state can facilitate the coupling of an excited state to the ground state, a process that kinetically competes with bimolecular deactivation by oxygen. Likewise, the intermolecular phenomenon is often

* To whom correspondence should be addressed. E-mail: progilby@chem.au.dk.

10.1021/jp905728d CCC: $40.75
Published on Web 08/24/2009

discussed in terms of an increase in the extent to which the M-O_2 CT state facilitates mixing of a higher-lying valence state of the encounter complex [e.g., $^3M_1\cdots O_2(X^3\Sigma_g^-)$] with the ground state [i.e., $^1M_0\cdots O_2(X^3\Sigma_g^-)$] at the expense of populating the $^1M_0\cdots O_2(a^1\Delta_g)$ state.[4,16] In cases that promote more CT character (e.g., polar solvents and M with a low oxidation potential), this effect is generally more pronounced.[9,20,22]

This adverse effect of CT character on $O_2(a^1\Delta_g)$ yields has been particularly pertinent in a problem of current interest: the two-photon photosensitized production of $O_2(a^1\Delta_g)$.[23,24] In this case, where sensitizer (i.e., M) excitation occurs as a consequence of the simultaneous absorption of two photons, intramolecular CT character is generally conducive for large transition moments. However, such CT character, combined with the fact that such molecules are usually also predisposed to have more M-O_2 CT character, translates into poor $O_2(a^1\Delta_g)$ yields. Therefore, in designing and optimizing efficient two-photon $O_2(a^1\Delta_g)$ sensitizers, the counteracting role(s) of CT must be carefully considered.

It has also been shown that $O_2(a^1\Delta_g)$ can be produced in appreciable yield upon irradiation into the M-O_2 CT absorption band. This was originally demonstrated with molecules used as solvents and, most interestingly, included molecules that do not have π-based chromophores (e.g., cyclohexane, methanol).[25−27] It was subsequently shown that $O_2(a^1\Delta_g)$ could also be produced upon irradiation into the M-O_2 CT absorption band of a solute molecule M dissolved in a given solvent.[9,28−30] These results have particular significance because they demonstrate an independent method by which one can access excited states of the M-O_2 complex, complementing methods based on the irradiation of a chromophore localized on M alone. In turn, through such independent techniques, one can achieve greater mechanistic insight into issues related to the mixing of M-O_2 states.

In this context, it is also pertinent to note that for many molecules direct irradiation into the M-O_2 CT band results in the oxygenation of M with products that are not otherwise obtained by irradiation of a transition localized on M alone.[31−34] In a wonderful extension of this phenomenon, Blatter and Frei[35,36] demonstrated that when present in a zeolite cavity, the M-O_2 CT state can be sufficiently stabilized such that irradiation in the visible region of the spectrum can likewise result in the unique CT-dependent oxygenation of M. These latter experiments can have many practical applications, particularly with the use of solar energy to selectively modify hydrocarbons.[37]

Despite its fundamental importance in numerous chemical systems, the extent of interaction/coupling between the CT state and other states of the M-O_2 complex is, surprisingly, still a matter of debate. Many issues remain unsettled, particularly those pertinent for a thorough discussion of oxygen-induced deactivation of an excited state of M. Part of the problem can be traced to poor and inaccurate data, particularly from experiments in which the effects of M-O_2 CT excitation were examined without the proper controls.

On this basis, we set out to systematically and methodically reinvestigate a number of key, unresolved issues pertinent to the role of the CT state in the M-O_2 system. In particular, using the results of new, more extensive and accurate experiments, we wanted to instill a sense of confidence in the data recorded. With these results in hand, we can now provide a description of the M-O_2 system that conforms to Occam's razor: there is indeed a simple and generally applicable model that accounts for the effects of the M-O_2 CT state. From a wider perspective, the material provided herein also helps to elucidate how an intermolecular CT state can, in general, influence excited-state relaxation dynamics.

Historical Background. Because this is a "mature" topic, it is necessary to present a certain amount of more detailed background information to frame the problem properly.

1-Methylnaphthalene, MN, and 1-ethylnaphthalene, EN, have many features that make them useful molecules, M, for these studies, and they have been used extensively in the past.[9,29,30,38] The photophysical properties of EN mirror those of MN, justifying a direct comparison between the two molecules.[22] We have worked with MN[9,38] and opted to do so again for this study. It is a liquid at ambient temperature, and thus large quantities of MN are readily dissolved in a number of liquid solvents.[38] For the present work, we limited ourselves to the use of acetonitrile, ACN, and cyclohexane, CHX. ACN has a large static dielectric constant ($\varepsilon_{st} = 37.5$) and, as such, can be considered to be a polar solvent. CHX is not polar ($\varepsilon_{st} = 2.0$). With respect to the high-frequency dielectric response, CHX is slightly more polarizable than ACN, as reflected in their refractive indices [n_D(CHX) = 1.423 and n_D(ACN) = 1.344, both at 20 °C]. These two solvents have likewise been used in past studies of the M-O_2 system.[9,29,30]

The addition of large amounts of MN to another liquid is often a required component in a study of the MN-O_2 system, certainly for experiments in which excited states are populated via irradiation into the MN-O_2 CT absorption band (vide infra). The addition of MN to ACN and CHX at these concentrations causes appreciable changes in properties of the entire sample that, in turn, can influence experiments performed to characterize the MN-O_2 system. For example, the dielectric properties of a 2 M solution of MN in CHX are significantly different from those of neat CHX. Although aspects of this issue have been addressed in previous studies, the use of such solvent mixtures has, in general, compromised and limited the accuracy of earlier work. A key and unique component of our present study is that data have been systematically recorded as a function of the MN concentration, and the results have been interpreted accordingly.

Direct Charge-Transfer Excitation. Because large amounts of MN can be added to both ACN and CHX, one can obtain an appreciably large absorbance for the MN-O_2 CT band at 355 nm. The latter is coincident with the third harmonic of a Nd:YAG laser, which facilitates a number of different experiments. Importantly, at this wavelength, there is no competing CT absorption due to complexes between oxygen and either ACN or CHX because these bands are further in the UV.[38] Therefore, at 355 nm, one can exclusively irradiate into the MN-O_2 CT band. Eventually, a fraction of the initially excited CT complexes will decay to ultimately produce $O_2(a^1\Delta_g)$, which can be spectroscopically detected by its characteristic near-IR phosphorescence centered at ~1270 nm.[9,29,30] This fraction is embodied in the $O_2(a^1\Delta_g)$ quantum yield obtained upon excitation into the CT channel, Φ_Δ^{CT}.

We now consider an M-O_2 energy level diagram with specific reference to MN (Figure 2). We make the reasonable assumption that the energy of a given state of the MN-O_2 complex principally reflects the energies of the isolated molecules. This assumption is consistent with spectroscopic data that show minimal complex-dependent energy perturbations.[16,39,40] A more complete discussion of the relative energetics of M-O_2 states, particularly with reference to the effects of state mixing, can be found in the article by Paterson et al.[16]

The energies of $O_2(a^1\Delta_g)$ and $^3MN_1$, 94 and 254 kJ/mol, respectively, are established.[45,46] The energy of $^1MN_1$, 377 kJ/mol, is likewise established[45] and is sufficiently high as to

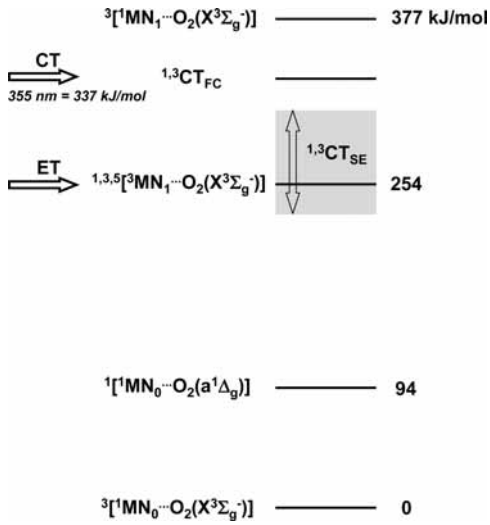

Figure 2. Energy diagram showing pertinent states of the MN$\cdots$O$_2$ photosystem.[41] For the interaction of two triplet states [i.e., $^3MN_1$ and $O_2(X^3\Sigma_g^-)$], spin states of singlet, triplet, and pentuplet multiplicity can be formed.[44] The region shaded in gray schematically shows the energy domain of the solvent-equilibrated CT states, $^{1,3}CT_{SE}$, the position of which depends on the solvent. The two independent excitation channels are indicated by horizontal arrows.

preclude its formation under the conditions employed in the present study. The molar energy of our 355 nm pulsed laser used to irradiate the MN-O$_2$ CT band is 337 kJ/mol. This process results in the production of the CT Franck−Condon state, denoted with the subscript FC in Figure 2. Because the ground-state MN-O$_2$ complex is a triplet spin state, the CT state initially populated will also be a triplet, $^3CT_{FC}$. However, this state is in rapid equilibrium with the corresponding singlet state, $^1CT_{FC}$. For the present study, it is reasonable to consider these states to be energetically degenerate.

In this study, it is essential to distinguish between the Franck−Condon CT states, $^{1,3}CT_{FC}$, and the lower-energy solvent-equilibrated CT states, $^{1,3}CT_{SE}$. (We likewise consider the singlet and triplet CT_{SE} states to be degenerate and in rapid equilibrium.) The energy of the $^{1,3}CT_{SE}$ states depends on the solvent and, at the appropriate limit of [MN] $\rightarrow$ 0, will certainly be quite different for the two solvents used in the present study. The effective energy range is depicted qualitatively by the region shaded in gray in Figure 2. A quantitative assessment of the CT_{SE} energy can be obtained through the use of eq 1.[47]

$$\Delta G^{CT} = F(E^{ox}_{MN} - E^{red}_{O_2}) - E_T + C \qquad (1)$$

Here ΔG^{CT} is the change in Gibbs energy relative to that of the MN triplet state, E_T. F is Faraday's constant and $E_{MN}{}^{ox}$ and $E_{O_2}{}^{red}$ are oxidation and reduction potentials for MN and O$_2$, respectively. Equation 1 also contains a Coulombic interaction term, C, which depends on the dielectric properties of the solvent and the interaction distance between the MN radical cation, $MN^{\bullet+}$, and the superoxide anion, $O_2^{\bullet-}$.

In CHX, the $^{1,3}CT_{SE}$ states are estimated to be substantially higher in energy than the MN triplet state, and the energy difference between the $^{1,3}CT_{FC}$ and $^{1,3}CT_{SE}$ states will be comparatively small. In turn, the $^{1,3}CT_{FC}$ states are expected to couple very strongly to the $^{1,3}CT_{SE}$ states in CHX. In ACN, which has a comparatively short solvent reorientation time (<1 ps)[38,48] and a large dipole moment ($\varepsilon_{st} = 37.5$), the $^{1,3}CT_{SE}$ states ($\tau \approx 10$ ps[29,30]) will be effectively stabilized and have an energy less than that of the MN triplet state. (Application of eq 1 yields a MN-O$_2$ CT_{SE} energy that is ~30−40 kJ/mol lower than that of the MN triplet state.[30,47]) Therefore, in ACN, the initially formed $^{1,3}CT_{FC}$ states should be able to couple to both the $^{1,3}CT_{SE}$ and $^3MN_1\cdots O_2(X^3\Sigma_g^-)$ states. This could be manifested in a smaller value for $\Phi_\Delta{}^{CT}$ in ACN than in CHX because one could, in ACN, "bypass" the MN triplet state by relaxing directly to the lower-energy $^{1,3}CT_{SE}$ states, which, in turn, could then couple to the MN-O$_2$ ground state.

It is in such statements that the crux of the problem lies. What is the relative extent to which the $^{1,3}CT_{FC}$ states couple to the $^{1,3}CT_{SE}$ and $^3MN_1\cdots O_2(X^3\Sigma_g^-)$ states? Can the $^1CT_{SE}$ state directly couple to the $^1MN_0\cdots O_2(a^1\Delta_g)$ state and, as such, be an immediate precursor to $O_2(a^1\Delta_g)$? Or is the $^3MN_1\cdots O_2(X^3\Sigma_g^-)$ state always the $O_2(a^1\Delta_g)$ precursor?

Sensitized Production of ^3MN. To address further the role of the $^{1,3}CT_{SE}$ states in the production of $O_2(a^1\Delta_g)$, one can choose an alternative and independent excitation channel wherein the MN triplet state is selectively and quantitatively generated via energy-transfer (ET) from the triplet state of an aromatic ketone, K (eq 2). To preclude competing hydrogen abstraction reactions with the solvent, the ketone of choice for experiments performed in CHX is *p*-methoxyacetophenone.[9] In ACN, benzophenone is also an acceptable ketone to use.[9] We refer to this as the ET excitation channel (Figure 2) and denote the $O_2(a^1\Delta_g)$ quantum yield obtained via this channel $\Phi_\Delta{}^{ET}$.

$$^1K_0 \xrightarrow{h\nu} {}^1K_1 \xrightarrow{\Phi_{isc} = 1} {}^3K_1 \xrightarrow{^1MN_0} {}^1K_0 + {}^3MN_1 \qquad (2)$$

To complement the $O_2(a^1\Delta_g)$ quantum yield determinations and to help decouple the behavior of the MN triplet state from that of the $^{1,3}CT_{SE}$ states, one can also use triplet absorption measurements to obtain the quantum yields of the MN triplet state formation via the two excitation channels (i.e., $\Phi_T{}^{CT}$ and $\Phi_T{}^{ET}$).

The $O_2(a^1\Delta_g)$ quantum yield following oxygen quenching of a triplet state sensitizer is given by eq 3.

$$\Phi_\Delta = \Phi_T f_T^{O_2} S_\Delta \qquad (3)$$

Here $f_T{}^{O_2}$ is the fraction of triplet states quenched by oxygen and S_Δ is the fraction of these quenching events that result in $O_2(a^1\Delta_g)$ formation. The parameter $f_T{}^{O_2}$ can be determined by recording the sensitizer triplet-state lifetimes in the absence and presence of oxygen. For the present study, we extract pertinent photophysical quantities under conditions where $f_T{}^{O_2} = 1$. With this is mind, let us now consider our case in ACN where the energy of the $^3MN_1$ state is greater than that of the $^{1,3}CT_{SE}$ states. Assuming that (i) $^3MN_1$ can relax to produce the $^{1,3}CT_{SE}$ states and (ii) both the $^3MN_1$ and $^1CT_{SE}$ states can act as immediate precursors to $O_2(a^1\Delta_g)$, then eq 4 defines the relationship between the observed $O_2(a^1\Delta_g)$ quantum yield and the contributions from these two channels.

$$\Phi_\Delta = \Phi_T S_{\Delta,T} + \Phi_T f_T^{CT} S_{\Delta,CT} = \Phi_T (S_{\Delta,T} + f_T^{CT} S_{\Delta,CT}) \qquad (4)$$

That is

$$S_{\Delta} = S_{\Delta,T} + f_T^{CT} S_{\Delta,CT} \quad (5)$$

In these equations, f_T^{CT} quantifies the fraction of $^3MN_1$ states that relax to produce the $^{1,3}CT_{SE}$ states and $S_{\Delta,CT}$ represents the fraction of CT_{SE} states yielding $O_2(a^1\Delta_g)$. Therefore, the first term in eq 5 quantifies the extent to which $^3MN_1$ is the immediate $O_2(a^1\Delta_g)$ precursor, whereas the second term quantifies the amount of $O_2(a^1\Delta_g)$ produced directly from the $^{1,3}CT_{SE}$ states.

Summary of Previous Results. Disagreement persists in the literature on the fate of the MN-O_2 $^{1,3}CT_{FC}$ states and the extent to which the $^1CT_{SE}$ state plays a role as an immediate precursor in $O_2(a^1\Delta_g)$ production. To facilitate discussion of the data presented in the current work, we briefly summarize key results from previous studies (Table 1).

Kristiansen et al.[9] concluded that upon MN-O_2 CT excitation in CHX, subsequent relaxation generates the MN triplet state with a quantum efficiency of 1.0, and it is this latter state that is the sole immediate precursor to $O_2(a^1\Delta_g)$. In ACN, these authors observed that the $O_2(a^1\Delta_g)$ yield dropped significantly when exciting through the CT channel (i.e., $\Phi_{\Delta}^{ET}/\Phi_{\Delta}^{CT} > 1$ in ACN). This was attributed to a lower-energy, stabilized CT_{SE} state that could (i) better couple to the ground MN-O_2 state and (ii) possibly dissociate to form the solvated $MN^{\bullet+}$ and $O_2^{\bullet-}$ radical ions, processes that both provide a deactivation channel that competes with $O_2(a^1\Delta_g)$ formation. It was inferred that in ACN not all of the MN triplet states produced $O_2(a^1\Delta_g)$ (i.e., $S_{\Delta,T} < 1$) and that a fraction of the $O_2(a^1\Delta_g)$ population could still be directly produced from the CT_{SE} state (i.e., $S_{\Delta,CT} > 0$).

McGarvey et al.[30] examined the oxygen-dependent behavior of EN. These authors reported that in both CHX and ACN, not all EN triplet states decay to produce $O_2(a^1\Delta_g)$ (i.e., $S_{\Delta,T} < 1$). They confirmed that Φ_{Δ}^{CT} is indeed smaller in ACN than in CHX. To explain their Φ_{Δ}^{CT} data and to account for the notion that the triplet state of EN cannot be the sole precursor of $O_2(a^1\Delta_g)$, these authors proposed that upon irradiation into the M-O_2 CT band, $O_2(a^1\Delta_g)$ production can also occur via dissociation of a doubly excited MN$\cdots O_2$ complex produced from the $^{1,3}CT_{FC}$ states. This latter hypothesis differs significantly from that of Kristiansen et al.,[9] who inferred, rather, that the additional source of $O_2(a^1\Delta_g)$ will be the M-O_2 $^1CT_{SE}$ state.

In contrast, Logunov and Rodgers[29] reported that in both CHX and ACN the MN triplet state produces $O_2(a^1\Delta_g)$ with unit efficiency (i.e., $S_{\Delta,T} = 1$), and concluded that $^3MN_1$ is the only direct precursor to $O_2(a^1\Delta_g)$.

In summary, although there is some consistency in earlier publications on this photosystem, there are also clear and fundamental differences in both the data reported and the models used to interpret the data. We therefore set out to see if these differences could be reconciled.

Results and Discussion

Charger-Transfer Absorption Spectra. In Figure 3, we show absorption spectra for 1.66 M MN in ACN recorded under N_2- and O_2-saturated conditions. On the basis of previous work,[3,9,26] we assign this O_2-dependent absorption shoulder to the transition in which the MN-O_2 CT state is populated. Also shown in Figure 3 are plots of the absorbance of this CT transition at 355 nm as a function of the MN concentration in both ACN and CHX. The CT absorbance was obtained as the difference between O_2- and N_2-saturated solutions, thereby eliminating a possible artifact due to scattered light.[49] For all samples, the mole fraction of added MN was used to determine the concentration of MN. (See the Supporting Information).

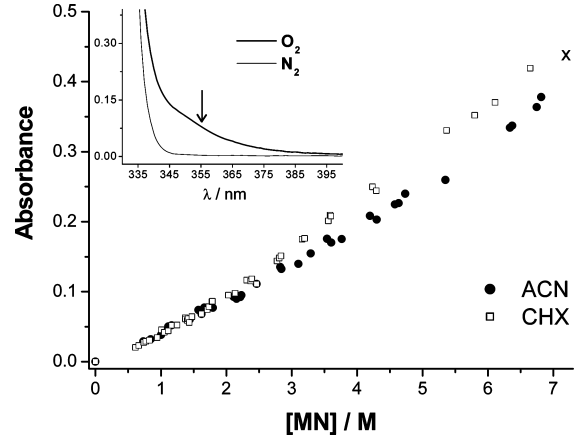

Figure 3. Plot of the MN-O_2 CT absorbance at 355 nm in both ACN and CHX. The data point marked with an × is for neat MN. The inset shows absorption spectra obtained under both O_2 and N_2 saturated conditions for 1.66 M MN dissolved in ACN, and the arrow indicates the 355 nm excitation wavelength used in our experiments.

According to the Beer−Lambert law, the MN-O_2 CT absorbance in a cell of path length z should be directly proportional to the concentration of the ground-state complex, $[^3[^1MN_0\cdots O_2(X^3\Sigma_g^-)]]$, which, in turn, is defined as the product of an equilibrium constant, K_{eq}, and the equilibrated concentrations of MN and oxygen (eq 6).[40]

$$A_{CT} = z\varepsilon_{CT}[^3[^1MN_0\cdots O_2(X^3\Sigma_g^-)]] = z\varepsilon_{CT}[^1MN_0]_{eq}[O_2(X^3\Sigma_g^-)]_{eq}K_{eq} \quad (6)$$

For both solvents, we observe a deviation from the Beer−Lambert linearity as the concentration of MN is increased (Figure 3). This may reflect a number of phenomena. First, it is likely that the solubility of O_2 in MN is not the same as that in ACN and CHX.[50,51] Therefore, an increase in the MN concentration will cause an incremental change in the amount of O_2 that can be dissolved. Second, recall that the refractive index of CHX (1.423) is greater than that of ACN (1.344) and, as such, CHX is more polarizable than ACN. This could contribute to a solvent-dependent difference in the stabilization of the MN-O_2 CT_{FC} state which, in turn, could also contribute to the difference between the CHX and the ACN data in Figure 3.[38] In any event, the data in Figure 3 clearly show that unless precautions are taken complications can arise in the interpretation of data obtained using high concentrations of MN in ACN and CHX.

Singlet Oxygen Quantum Yields. ***Cyclohexane.*** Figure 4 shows how the $O_2(a^1\Delta_g)$ quantum yield depends on the concentration of MN upon (a) selectively generating the $^3MN_1$ state in a triplet ketone sensitized reaction (Φ_{Δ}^{ET}, Figure 4a) and (b) direct excitation into the MN-O_2 CT band (Φ_{Δ}^{CT}, Figure 4b).

In the ketone-sensitized experiment, the concentration of *p*-methoxyacetophenone was such that the absorbance of this molecule at 355 nm was much higher than that for the MN-O_2 CT transition. As such, all incident photons were absorbed by *p*-methoxyacetophenone. In this experiment, the $O_2(a^1\Delta_g)$ quantum yield decreases slightly as the MN concentration is increased (Figure 4a). This result could reflect the process wherein $^3MN_1$ produced by energy transfer from the triplet ketone is, itself, quenched by ground-state MN (eq 7). In turn,

TABLE 1: Measurements of $O_2(a^1\Delta_g)$ Yields Using Two Separate Channels to Access MN-O_2 Excited States in Cyclohexane (CHX) and Acetonitrile (ACN).[a]

	Φ_Δ^{ET}	Φ_Δ^{CT}	$\Phi_\Delta^{ET}/\Phi_\Delta^{CT}$	Φ_T^{CT}	S_Δ
			CHX		
current work	0.86 ± 0.04	0.78 ± 0.08	1.10 ± 0.12	0.81 ± 0.07	0.86 ± 0.04
Kristiansen et al.[9]	($\sim$1)	(0.91 ± 0.11)	1.00 ± 0.04	(0.91 ± 0.11)	($\sim$1)
McGarvey et al.[30]	0.86 ± 0.09[b]	0.78 ± 0.08[b]	1.10 ± 0.16[b]	0.80 ± 0.08[b]	0.86 ± 0.09[b]
	0.84 ± 0.08[c]				0.84 ± 0.08[c]
Logunov et al.[29,d]	1.0 ± 0.1	0.87 ± 0.1	(1.15 ± 0.18)	1.0 ± 0.1	1.0 ± 0.1
			ACN		
current work	0.65 ± 0.03	0.33 ± 0.02	1.97 ± 0.15	0.35 ± 0.03	$\sim 0.62 \pm 0.06$[e]
Kristiansen et al.[9]			1.52 ± 0.05		(<1)
McGarvey et al.[30]	0.51 ± 0.05[b]	0.36 ± 0.04[b]	1.43 ± 0.21[b]	0.40 ± 0.04[b]	0.51 ± 0.05[b]
	0.60 ± 0.06[c]				0.60 ± 0.06[c]
Logunov et al.,[29,d]	1.05 ± 0.1	0.55 ± 0.1	(1.91 ± 0.39)	0.5 ± 0.1	1.05 ± 0.1

[a] Numbers in parentheses are not specifically reported in the papers cited but are calculated or inferred using information available in these papers. [b] Study performed using EN. CT experiments were performed using 1.5 M EN solutions and an ambient oxygen pressure of 2−4 atm. [c] Data obtained using MN.[22] [d] CT experiments were performed using 2 M MN solutions under oxygen-saturated conditions. [e] This value is the mean of S_Δ values that are restricted to the range 0.58 to 0.65. (See the Supporting Information).

at higher concentrations of MN, there would be less $^3MN_1$ available for quenching by $O_2(X^3\Sigma_g^-)$ and less $O_2(a^1\Delta_g)$ produced.

$$^3K_1 \xrightarrow{^1MN_0} {}^3MN_1 \xrightarrow{^1MN_0} {}^1MN_0 + {}^1MN_0$$
$$\downarrow{\scriptstyle O_2(X^3\Sigma_g^-)}$$
$$^1MN_0 + O_2(a^1\Delta_g) \qquad (7)$$

We have established that at [MN] $\approx$ 0.3 M (a) all of the *p*-methoxyacetophenone triplet states are quenched by $^1MN_0$ to yield $^3MN_1$ and (b) all $^3MN_1$ states thus produced are quenched by oxygen in an air-saturated solution (i.e., $f_T^{O_2} = 1$).[9] Admittedly, the apparent decrease seen in Φ_Δ^{ET} as [MN] is decreased to <0.1 M (Figure 4a) could reflect the fact that here quenching of the ^{3}ketone by oxygen can now more effectively compete with the desired quenching by $^1MN_0$. Therefore, as we extrapolate the Φ_Δ^{ET} data obtained to the limit of [MN] $\rightarrow$ 0, the resultant number, $\Phi_\Delta^{ET} = 0.86 \pm 0.04$, is likely best seen as a lower limit to the accurate value of Φ_Δ^{ET} in CHX as a consequence of the data point at [MN] < 0.1 M. In any event, any slight change in this CHX number does not have a significant consequence in the development and interpretation of our model for state coupling (vide infra).

In the case of $O_2(a^1\Delta_g)$ production following direct MN-O_2 CT excitation, we also observed a decrease in the $O_2(a^1\Delta_g)$ yield, Φ_Δ^{CT}, as the amount of MN in the sample was increased (Figure 4b). To ensure appreciable absorption of light by the MN-O_2 complex, we used MN concentrations over the range of 1.0 to 4.3 M. Although this decrease in the quantum yield can again be explained by eq 7, another phenomenon may also contribute to the data observed. Specifically, as the MN concentration is increased, the sample will increasingly have dielectric properties that reflect those of MN (i.e., larger static and optical dielectric constants). As such, we additionally propose that under these conditions the $^{1,3}CT_{SE}$ states will be better stabilized, which, in turn, will result in better coupling to the ground MN-O_2 state at the expense of $O_2(a^1\Delta_g)$ production (vide infra). In any event, we again chose the limiting value as [MN] $\rightarrow$ 0 (linear fit in Figure 4b) to report a number for the $O_2(a^1\Delta_g)$ quantum yield: $\Phi_\Delta^{CT} = 0.78 \pm 0.08$. As with our value for Φ_Δ^{ET}, this Φ_Δ^{CT} number agrees favorably with data reported by McGarvey et al.[30] (Table 1). In itself, this coincidence is remarkable considering the experiments performed in these respective studies and the fact that the data significantly depend on [MN].

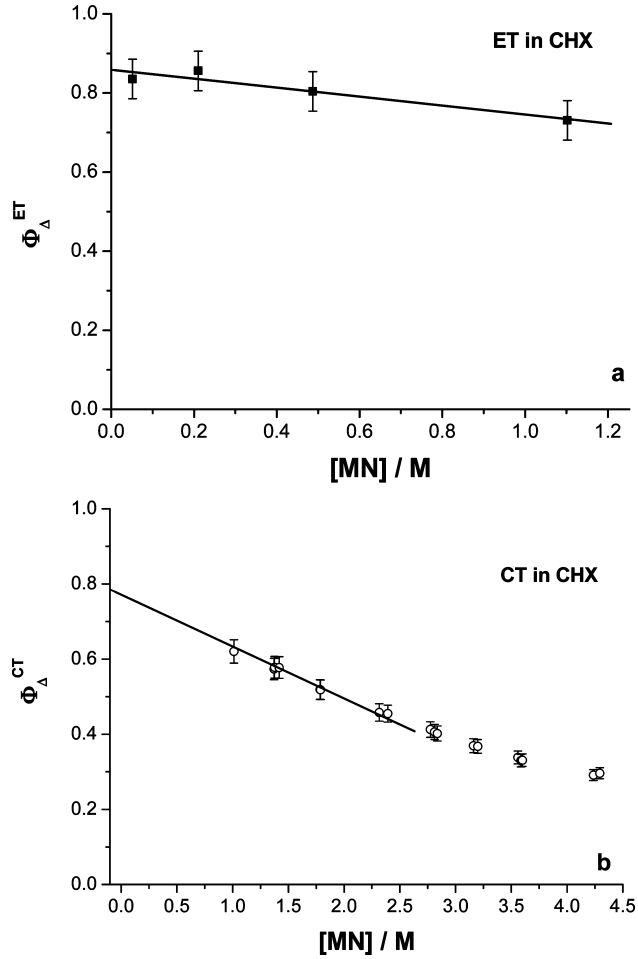

Figure 4. $O_2(a^1\Delta_g)$ quantum yields in CHX upon ET excitation (Φ_Δ^{ET}, panel a) and CT excitation (Φ_Δ^{CT}, panel b). Values of the respective quantum yields shown in Table 1 were obtained from the limit [MN] $\rightarrow$ 0. In panel b, the fit pertinent for this [MN] $\rightarrow$ 0 extrapolation was applied only to data at [MN] < 2.5 M, where it is expected that the effects shown in eq 7 dominate and that the data should indeed scale linearly with a change in [MN]. (See discussion in the text).

The ratio of the $O_2(a^1\Delta_g)$ quantum yields produced via the two complementary excitation channels is therefore $\Phi_\Delta^{ET}/\Phi_\Delta^{CT} = 1.10 \pm 0.12$ (Table 1). This finding agrees with those from several earlier reports and is consistent with a model in which

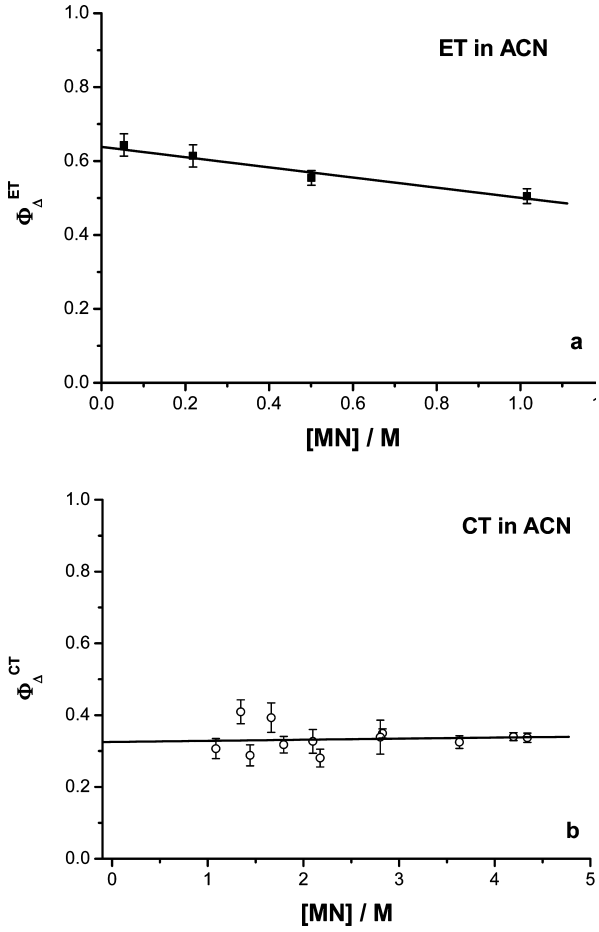

Figure 5. $O_2(a^1\Delta_g)$ quantum yields in ACN upon ET excitation (Φ_Δ^{ET}, panel a) and CT excitation (Φ_Δ^{CT}, panel b). Values of the respective quantum yields shown in Table 1 were obtained from the limit [MN] $\rightarrow$ 0.

in this solvent, the MN-O_2 $^1CT_{SE}$ state is not an immediate precursor of $O_2(a^1\Delta_g)$. Rather, because the magnitudes of Φ_Δ^{CT} and Φ_Δ^{ET} are similar, one would infer that once populated, the higher-energy $^{1,3}CT_{SE}$ states will efficiently relax to produce the lower-energy MN triplet state, which is then the immediate $O_2(a^1\Delta_g)$ precursor.

Acetonitrile. The corresponding $O_2(a^1\Delta_g)$ quantum yields obtained in ACN are shown in Figure 5, and the pertinent data are likewise presented in Table 1. To determine Φ_Δ^{ET}, we used benzophenone as the sensitizing ketone. As with the CHX data, we observe a slight decrease in the $O_2(a^1\Delta_g)$ yield as the MN concentration is increased. Again, we attribute this to quenching of $^3MN_1$ by $^1MN_0$ (eq 7).

It is imperative that in this solvent we obtain an accurate value of Φ_Δ^{ET} at the limit [MN] $\rightarrow$ 0. Therefore, we must independently ascertain that as [MN] is decreased <0.1 M, the deactivation of ^{3}benzophenone is still dominated by the MN quenching channel and not influenced by the O_2 quenching channel. As outlined in the Supporting Information, we have established through a series of triplet absorption experiments that the rate constant for ^{3}benzophenone deactivation by MN is $(1.11 \pm 0.05) \times 10^{10}$ s^{-1} M^{-1}. The rate constant for ^{3}benzophenone quenching by oxygen is 2.3×10^9 s^{-1} M^{-1}.[52] Therefore, in an air-saturated solution of 0.05 M MN in ACN, greater than 99% of the ^{3}benzophenone molecules produced are still quenched by MN. As such, the value of $\Phi_\Delta^{ET}(ACN) = 0.65 \pm 0.03$ obtained from the limit [MN] $\rightarrow$ 0 should be quite accurate.

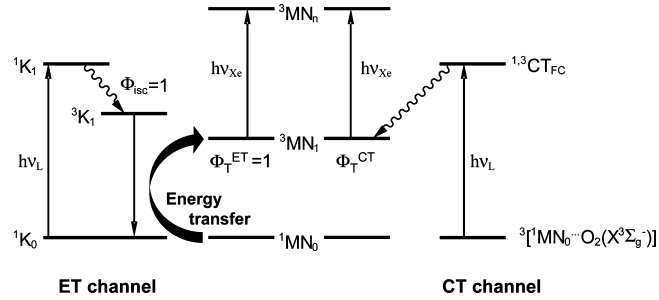

Figure 6. Schematic representation of the approach to determine $^3MN_1$ state quantum yields upon MN-O_2 CT excitation. ν_L and ν_{Xe} denote excitation using a pulsed nanosecond laser and a steady-state Xe lamp, respectively.

In contrast with the data obtained from CHX, the $O_2(a^1\Delta_g)$ yield obtained upon irradiation into the MN-O_2 CT band in ACN does not appreciably depend on the MN concentration (Figure 5b). This could reflect the fact that increasing the concentration of MN in ACN will not have as drastic an effect on the dielectric properties of the medium as increasing the concentration of MN in CHX. Therefore, there may not be a substantive [MN]-dependent change in the energy of the $^{1,3}CT_{SE}$ states in ACN, which, in turn, would mean that the extent of coupling between the $^{1,3}CT_{SE}$ and MN-O_2 ground states would remain [MN]-invariant in this solvent. In any event, the quantum yield obtained at the limit [MN] $\rightarrow$ 0 is $\Phi_\Delta^{CT} = 0.33 \pm 0.02$ (Table 1).

The measured quantities lead to a ratio of quantum yields obtained via the two excitation channels of $\Phi_\Delta^{ET}/\Phi_\Delta^{CT} = 1.97 \pm 0.15$. This ratio is two times larger than that found in the CHX experiments and principally reflects the fact that in ACN Φ_Δ^{CT} is significantly smaller than that in CHX (Table 1). These data are consistent with a model where, in ACN, the $^{1,3}CT_{FC}$ states do not efficiently couple to the $^3MN_1$ state. Rather, the $^{1,3}CT_{FC}$ states must preferentially couple to states that do not result in $O_2(a^1\Delta_g)$ production. This model is also consistent within the context of eq 7, where a decrease in the yield of $^3MN_1$ would indeed result in values of Φ_Δ^{CT} that are less dependent on the MN concentration (Figure 5b).

However, to substantiate this model further, it is necessary to quantify independently quantum yields for $^3MN_1$ formation following MN-O_2 CT excitation, Φ_T^{CT}, in both ACN and CHX.

Quantum Yields of the MN Triplet State. To determine Φ_T^{CT}, we compared the intensity of the $^3MN_1$ transient absorption signal obtained using the CT excitation channel to the corresponding signal obtained following ET excitation. For the latter, we know that in both ACN and CHX the $^3MN_1$ state is formed quantitatively from the sensitizing ketone (i.e., $\Phi_T^{ET} = 1$). As such, we can independently quantify the amount of $^3MN_1$ produced and thereby establish a standard. The approach is illustrated in Figure 6, and examples of the transient $^3MN_1$ absorption signals obtained in ACN are shown in Figure 7. (See the Supporting Information for corresponding data recorded in CHX).

In both the ET and CT excitation experiments, values that appropriately represent the amount of $^3MN_1$ produced can be obtained by fitting a single exponential decay to the data and extrapolating to time = 0 (Figure 7). In the MN-O_2 CT excitation experiment, the O_2-saturated conditions naturally yield a shorter $^3MN_1$ lifetime because of quenching by ground-state oxygen. The quantum yields of $^3MN_1$ formation upon CT excitation thus obtained are $\Phi_T^{CT} = 0.81 \pm 0.07$ in CHX and $\Phi_T^{CT} = 0.35 \pm 0.03$ in ACN (Table 1). Although our data are consistent with those of McGarvey et al.,[30] the numbers reported by Logunov and Rodgers[29] appear to be too large (albeit with a larger error as well).

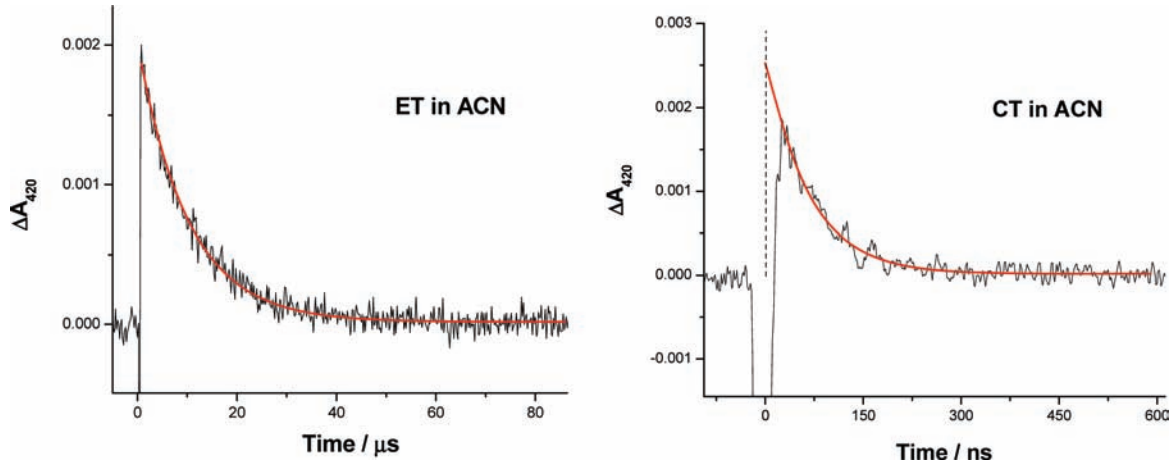

Figure 7. Observed $^3MN_1$ absorption signals in ACN using the ET excitation channel (left) and the CT channel (right). Data in the ET experiment were recorded under N_2-saturated conditions and, as such, yield a longer $^3MN_1$ lifetime. The data shown have not been normalized for differences in sample absorbance at the irradiation wavelength of 355 nm where A(CT) > A(ET) and hence ΔA_{420}(CT) > ΔA_{420}(ET).

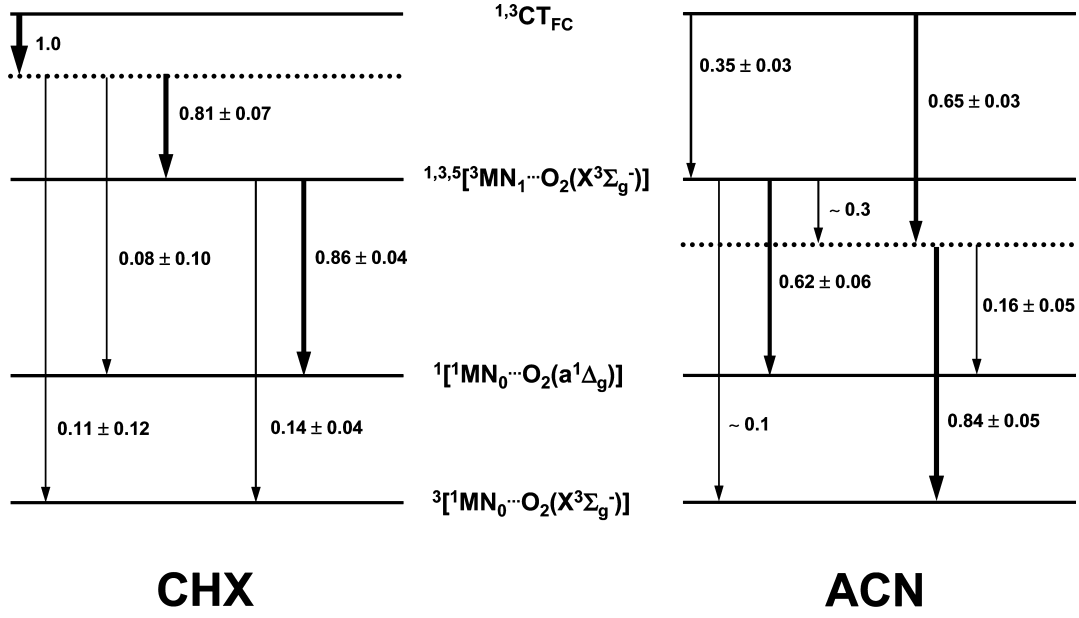

Figure 8. Proposed energy and coupling diagrams for the MN-O_2 photosystem in CHX (left) and ACN (right). In each solvent, characterized as a dielectric medium under the limiting condition [MN] → 0, the energetic position of the $^{1,3}CT_{SE}$ states is schematically indicated by the dotted line (•••). For a given state, the arrows indicate possible decay paths, and the number associated with a particular arrow indicates the fraction of that state that decays by that path. Details of how these numbers were obtained from the data in Table 1 are given in the Supporting Information.

These $^3MN_1$ absorption experiments thus provide data that further corroborate a model in which in ACN, the $^{1,3}CT_{FC}$ states do not efficiently couple to the $^3MN_1$ state.

Energy Diagrams and State Coupling. We are now in a position to address, on both qualitative and quantitative levels, the main question posed in the Introduction: what is the role of the M-O_2 CT state in the production of $O_2(a^1\Delta_g)$, and what is the associated influence of the solvent? More specifically, and referring to eqs 4 and 5, we are interested in ascertaining whether $O_2(a^1\Delta_g)$ can be produced directly from the M-O_2 $^1CT_{SE}$ state or if the localized M triplet state is the only immediate precursor to $O_2(a^1\Delta_g)$. The central parameter is therefore $S_{\Delta,CT}$; if $S_{\Delta,CT} > 0$, then the $^1CT_{SE}$ state can indeed act as an $O_2(a^1\Delta_g)$ precursor.

On the basis of the data obtained in the current study (Table 1), we are able to construct energy diagrams in which the extent of coupling between the various states of the MN-O_2 photosystem is specified (Figure 8). In Figure 8, the arrows indicate the possible decay paths of a given state, and the associated numbers indicate the fraction of that state that decays by the indicated path. (The width of the arrow also represents the relative fraction.) The details of how these specific numbers were obtained from the data in Table 1 are given in the Supporting Information.

Focusing first on events in CHX, we find that the MN triplet state is more effectively coupled to $O_2(a^1\Delta_g)$ than to the ground MN-O_2 state (embodied in $\Phi_\Delta^{ET} = S_\Delta = 0.86$). Assuming that the $^{1,3}CT_{FC}$ states relax quantitatively to the comparatively high energy $^{1,3}CT_{SE}$ states, it now follows that these latter states, in turn, couple mainly to the MN triplet state ($\Phi_T^{CT} = 0.81$).[53] It is significant to note that within our model a small fraction of the $^{1,3}CT_{SE}$ states indeed appear to couple directly to the $O_2(a^1\Delta_g)$ state (i.e., $S_{\Delta,CT} = 0.08 \pm 0.10$). Admittedly, within the errors established by our data, we cannot exclude a value of $S_{\Delta,CT} \approx 0$. However, on the basis of the data obtained in ACN (vide infra), it is not unreasonable to consider that even in CHX the $^1CT_{SE}$ state could be a direct, albeit very minor, precursor of $O_2(a^1\Delta_g)$.

Turning now to ACN, a solvent in which the $^{1,3}CT_{SE}$ states are substantially stabilized, the observed value of $\Phi_T^{CT} = 0.35$ immediately implies that the $^{1,3}CT_{FC}$ states are now less strongly coupled to the $^{1,3}CT_{SE}$ states. The data indicate that roughly one-third of the $^{1,3}CT_{FC}$ states relax directly to the MN triplet state. Furthermore, the data indicate that the primary fate of the MN triplet state is the production of $O_2(a^1\Delta_g)$, just as in CHX. However, to account for the observed quantum yield of $\Phi_\Delta^{CT} = 0.33$, the $^{1,3}CT_{SE}$ states must play a significant role in the relaxation dynamics; although the main fate of the $^{1,3}CT_{SE}$ states is decay to the ground MN-O_2 state (84%), a significant fraction of these states (16%) must be a direct precursor to $O_2(a^1\Delta_g)$.

Several important conclusions can be drawn from the data summarized in Figure 8. Most importantly, we find that the $^1CT_{SE}$ state can indeed act as an immediate precursor to $O_2(a^1\Delta_g)$, particularly in ACN (i.e., $S_{\Delta,CT} > 0$). This conclusion is in sharp contrast with that of Logunov and Rodgers,[29] who claim that in all cases the immediate precursor to $O_2(a^1\Delta_g)$ is always the free triplet state of MN. One origin for this discrepancy is that the conclusions of Logunov and Rodgers were based on data with comparatively large error bars, and, as such, it was arguably difficult to discern accurately whether $S_{\Delta,CT}$ was greater than 0.

In interpreting their data in ACN, McGarvey et al.[30] likewise concluded that dynamic quenching of the $^3MN_1$ state by $O_2(X^3\Sigma_g^-)$ cannot be the sole immediate precursor to $O_2(a^1\Delta_g)$; as such, their conclusions also go against those of Logunov and Rodgers. However, in contrast with our model, as shown in Figure 8, McGarvey et al.[30] speculated that upon MN-O_2 CT excitation the additional channel for $O_2(a^1\Delta_g)$ formation first involves the coupling of the $^{1,3}CT_{FC}$ states to a doubly excited state, consisting of both $^3MN_1$ and $O_2(a^1\Delta_g)$. This doubly excited state could then dissociate to yield $O_2(a^1\Delta_g)$.[54]

When considering our data and those of McGarvey et al.,[30] the problem then reduces, once again, to ascertaining what is the immediate precursor to $O_2(a^1\Delta_g)$: in this case, the $^1CT_{SE}$ state or a doubly excited $^3MN_1$-$O_2(a^1\Delta_g)$ state. The energy of the $^3MN_1$ state is 254 kJ/mol,[45] and that of $O_2(a^1\Delta_g)$ is 94 kJ/mol.[16,46] This would require the proposed doubly excited state to have an energy of 348 kJ/mol. However, this energy of 348 kJ/mol is appreciably higher than the excitation energy associated with the 355 nm laser pulses used in the experiments (337 kJ/mol). Indeed, this concern was also expressed by McGarvey et al. in their own discussion. In any event, one must certainly consider it to be improbable that (i) the short-lived $^{1,3}CT_{FC}$ states will acquire ~11 kJ/mol from the thermal bath (note kT at room temperature ≈ 2.5 kJ/mol) and thereafter (ii) produce $O_2(a^1\Delta_g)$ with a quantum efficiency of 16%. Rather, we find our model shown in Figure 8 to be more reasonable. In short, the $^1CT_{SE}$ state must be a direct precursor to $O_2(a^1\Delta_g)$.

Conclusions

The data obtained in the current work clearly demonstrate that the intermolecular charge-transfer state between oxygen, O_2, and an organic molecule, M, can significantly influence the photophysics of the M-O_2 system. In particular, the CT state plays an important role in events that result in the photosensitized production of $O_2(a^1\Delta_g)$ and, indeed, can even be an immediate precursor of $O_2(a^1\Delta_g)$. This latter conclusion has been somewhat elusive over the past ~20 years and, for the well-studied system of 1-methylnaphthalene and oxygen, can only now be made with certainty on the basis of meticulous and systematic experiments. The results obtained and the model we propose conform to straightforward and standard arguments based on state mixing. In turn, this work illustrates a number of fundamental issues pertinent to the solvent-dependent dynamics of CT-mediated excited-state relaxation.

Experimental Section

Singlet Oxygen Quantum Yields. The time-resolved instrumentation and approach used to detect $O_2(a^1\Delta_g)$ by its 1270 nm phosphorescence have been described elsewhere.[55] We obtained quantum yields of $O_2(a^1\Delta_g)$ production following either CT-excitation, Φ_Δ^{CT}, or energy transfer from a ketone to produce the MN triplet state selectively, Φ_Δ^{ET}, by monitoring the intensities of the time-resolved $O_2(a^1\Delta_g)$ phosphorescence signals. This was done relative to the reference sensitizer perinaphthenone, PN, for which we used $\Phi_\Delta(ACN) = 0.99 \pm 0.03$ and $\Phi_\Delta(CHX) = 0.95 \pm 0.03$.[56,57]

The time-resolved $O_2(a^1\Delta_g)$ phosphorescence signal, which in all cases followed first-order decay kinetics, was integrated and normalized by the observed lifetime, the radiative rate constant, and the solvent refractive index.[9,58] These are important corrections given (1) the rather high concentrations of MN used in this work and (2) the fact that these photophysical and macroscopic properties depend on the MN concentration used. (See the Supporting Information).

For each quantum yield reported, a minimum of four samples with absorbance at 355 nm ranging from 0.03 to 0.30 were examined. For each sample, the corrected $O_2(a^1\Delta_g)$ signal was recorded for at least five different laser intensities over the range of $I = 4-40$ mW/cm^2, and a plot of this corrected signal as a function of I yielded a straight line, as expected. The slope of this line was then plotted as a function of the sample absorbance.[59] This procedure was duplicated for the reference sensitizer PN to yield relative values for Φ_Δ. The data ultimately reported are an average obtained by repeating this procedure at least three independent times.

Lifetimes obtained from the time-resolved $O_2(a^1\Delta_g)$ signals in neat liquids were ~80 μs in ACN, ~24 μs in CHX, and ~6.3 μs in MN, which is consistent with what is expected for these solvents.[19,60]

Refractive index measurements were performed at 20 °C using a Bellingham & Stanley refractometer with a sodium lamp as the light source. The refractive indexes measured for the neat liquids all agreed with literature values: $n_{ACN} = 1.3442 \pm 0.0002$, $n_{CHX} = 1.4266 \pm 0.0002$, and $n_{MN} = 1.6158 \pm 0.0003$. In both solvents, the refractive index was determined as a function of the MN concentration, and a linear correlation was found (Supporting Information). Such plots were used when correcting the $O_2(a^1\Delta_g)$ intensities (vide supra).

Triplet Absorption Experiments. The features of the instrumentation used to monitor time-resolved triplet absorption data are presented elsewhere.[55] The triplet spectrum of MN has a band maximum at 420 nm, and the pertinent time-resolved data were recorded at this wavelength.

Relative experiments to quantify triplet yields upon MN-O_2 CT excitation were performed in the following way. (See Figures 6 and 7.) For a given solvent, a solution of MN at a specified concentration was saturated with oxygen ([MN] > 1.0 M). We then recorded the resultant transient MN triplet absorption signal produced upon MN-O_2 CT excitation at 355 nm. For the corresponding ET excitation experiments, solutions of MN identical to those used in the CT experiments were prepared. A known amount of ketone was then added such that the ketone was the sole absorber at 355 nm. We subsequently removed oxygen by gently purging the solution with nitrogen gas for approximately 15 min. The MN triplet transient absorption signal was then recorded following

excitation of the ketone at 355 nm. The laser power was kept constant during these separate experiments. Because the MN triplet quantum yield in the ET excitation scheme is unity ($\Phi_T^{ET} = 1$), the triplet quantum yield following MN-O_2 CT excitation, Φ_T^{CT}, is easily obtained by relating the intensities of the respective signals. This approach has the advantage that the MN triplet-state extinction coefficient, which is known to change with the MN concentration, cancels out because the MN concentration is the same in the two experiments. For each solvent, a minimum of five samples with different MN concentrations were prepared, and, for each sample, Φ_T^{CT} was determined. The reported number and associated error is the statistical average of these experiments.

Materials. Acetonitrile, cyclohexane (both Aldrich spectroscopic grade), and perinaphthenone (97%, Aldrich) were used as received. Benzophenone and *p*-methoxyacetophenone were recrystallized twice from MeOH and dried prior to use. 1-Methylnaphthalene (97%, Fluka) was filtered through silica gel immediately before use. This latter procedure is a crucial component of this study because MN readily degrades, even in the dark and under nitrogen. All experiments were performed and all data were recorded under conditions where after the experiment there was no evidence of MN degradation (as determined by UV/vis spectroscopy). Fresh samples of MN were routinely used.

Acknowledgment. This work was supported by the Danish National Research Foundation through a block grant for the Center for Oxygen Microscopy and Imaging.

Supporting Information Available: Evaluation of $O_2(a^1\Delta_g)$ phosphorescence signals, refractive index of MN solutions as a function of MN concentration, $O_2(a^1\Delta_g)$ lifetimes and Stern−Volmer plots of $O_2(a^1\Delta_g)$ quenching by MN, MN triplet absorption signals in CHX, quenching of the ketone triplet state by MN, and calculations for the energy and coupling diagrams for MN-O_2 in CHX and ACN. This material is available free of charge via the Internet at http://pubs.acs.org.

References and Notes

(1) Evans, D. F. *J. Chem. Soc.* **1953**, 345–347.
(2) Evans, D. F. *J. Chem. Soc.* **1957**, 1351–1357.
(3) Tsubomura, H.; Mulliken, R. S. *J. Am. Chem. Soc.* **1960**, *82*, 5966–5974.
(4) Kawaoka, K.; Khan, A. U.; Kearns, D. R. *J. Chem. Phys.* **1967**, *46*, 1842–1853.
(5) Khan, A. U.; Kearns, D. R. *J. Chem. Phys.* **1968**, *48*, 3272–3275.
(6) Garner, A.; Wilkinson, F. *Chem. Phys. Lett.* **1977**, *45*, 432–435.
(7) Redmond, R. W.; Braslavsky, S. E. *Chem. Phys. Lett.* **1988**, *148*, 523–529.
(8) Schmidt, R.; Shafii, F.; Schweitzer, C.; Abdel-Shafi, A. A.; Wilkinson, F. *J. Phys. Chem. A* **2001**, *105*, 1811–1817.
(9) Kristiansen, M.; Scurlock, R. D.; Iu, K.-K.; Ogilby, P. R. *J. Phys. Chem.* **1991**, *95*, 5190–5197.
(10) Ogilby, P. R.; Sanetra, J. *J. Phys. Chem.* **1993**, *97*, 4689–4694.
(11) Monroe, B. M. *J. Phys. Chem.* **1977**, *81*, 1861–1864.
(12) Ogryzlo, E. A.; Tang, C. W. *J. Am. Chem. Soc.* **1970**, *92*, 5034–5036.
(13) Clennan, E. L.; Noe, L. J.; Szneler, E.; Wen, T. *J. Am. Chem. Soc.* **1990**, *112*, 5080–5085.
(14) Stevens, B. *J. Photochem.* **1974/75**, *3*, 393–401.
(15) Stevens, B.; Small, R. D. *Chem. Phys. Lett.* **1979**, *61*, 233–238.
(16) Paterson, M. J.; Christiansen, O.; Jensen, F.; Ogilby, P. R. *Photochem. Photobiol.* **2006**, *82*, 1136–1160.
(17) Minaev, B. F.; Lunell, S.; Kobzev, G. I. *THEOCHEM* **1993**, *284*, 1–9.
(18) Minaev, B. F.; Ågren, H. *J. Chem. Soc., Faraday Trans.* **1997**, *93*, 2231–2239.
(19) Schweitzer, C.; Schmidt, R. *Chem. Rev.* **2003**, *103*, 1685–1757.
(20) McGarvey, D. J.; Szekeres, P. G.; Wilkinson, F. *Chem. Phys. Lett.* **1992**, *199*, 314–319.
(21) Flors, C.; Ogilby, P. R.; Luis, J. G.; Grillo, T. A.; Izquierdo, L. R.; Gentili, P.-L.; Bussotti, L.; Nonell, S. *Photochem. Photobiol.* **2006**, *82*, 95–103.
(22) Wilkinson, F.; McGarvey, D. J.; Olea, A. F. *J. Phys. Chem.* **1994**, *98*, 3762–3769.
(23) Frederiksen, P. K.; McIlroy, S. P.; Nielsen, C. B.; Nikolajsen, L.; Skovsen, E.; Jørgensen, M.; Mikkelsen, K. V.; Ogilby, P. R. *J. Am. Chem. Soc.* **2005**, *127*, 255–269.
(24) Nielsen, C. B.; Johnsen, M.; Arnbjerg, J.; Pittelkow, M.; McIlroy, S. P.; Ogilby, P. R.; Jørgensen, M. *J. Org. Chem.* **2005**, *70*, 7065–7079.
(25) Scurlock, R. D.; Ogilby, P. R. *J. Am. Chem. Soc.* **1988**, *110*, 640–641.
(26) Scurlock, R. D.; Ogilby, P. R. *J. Phys. Chem.* **1989**, *93*, 5493–5500.
(27) Ogilby, P. R.; Kristiansen, M.; Clough, R. L. *Macromolecules* **1990**, *23*, 2698–2704.
(28) Logunov, S. L.; Rodgers, M. A. J. *J. Phys. Chem.* **1992**, *96*, 2915–2917.
(29) Logunov, S. L.; Rodgers, M. A. J. *J. Phys. Chem.* **1993**, *97*, 5643–5648.
(30) McGarvey, D. J.; Wilkinson, F.; Worrall, D. R.; Hobley, J.; Shaikh, W. *Chem. Phys. Lett.* **1993**, *202*, 528–534.
(31) Hashimoto, S.; Akimoto, H. *J. Phys. Chem.* **1986**, *90*, 529–532.
(32) Hashimoto, S.; Akimoto, H. *J. Phys. Chem.* **1989**, *93*, 571–577.
(33) Onodera, K.; Furusawa, G.; Kojima, M.; Tsuchiya, M.; Aihara, S.; Akaba, R.; Sakuragi, H.; Tokumaru, K. *Tetrahedron* **1985**, *41*, 2215–2220.
(34) Kojima, M.; Sakuragi, H.; Tokumaru, K. *Bull. Chem. Soc. Jpn.* **1987**, *60*, 3331–3336.
(35) Blatter, F.; Frei, H. *J. Am. Chem. Soc.* **1993**, *115*, 7501–7502.
(36) Blatter, F.; Frei, H. *J. Am. Chem. Soc.* **1994**, *116*, 1812–1820.
(37) Frei, H.; Blatter, F.; Sun, H. *CHEMTECH* **1996**, 24–30.
(38) Kuriyama, Y.; Ogilby, P. R.; Mikkelsen, K. V. *J. Phys. Chem.* **1994**, *98*, 11918–11923.
(39) Ogilby, P. R. *Acc. Chem. Res.* **1999**, *32*, 512–519.
(40) Gooding, E. A.; Serak, K. R.; Ogilby, P. R. *J. Phys. Chem.* **1991**, *95*, 7868–7871.
(41) As in Figure 1, we have chosen to neglect the complex between ground-state MN and $O_2(b^1\Sigma_g^+)$; it is now well established that if the $O_2(b^1\Sigma_g^+)$ state is indeed formed, then it will rapidly deactivate in a collision complex to form the $O_2(a^1\Delta_g)$ state with unit efficiency.[19,42,43]
(42) Scurlock, R. D.; Wang, B.; Ogilby, P. R. *J. Am. Chem. Soc.* **1996**, *118*, 388–392.
(43) Bodesheim, M.; Schmidt, R. *J. Phys. Chem. A* **1997**, *101*, 5672–5677.
(44) Gijzeman, O. L. J.; Kaufman, F.; Porter, G. *J. Chem. Soc., Faraday Trans. II* **1973**, *69*, 708–720.
(45) Murov, S. L.; Carmichael, I.; Hug, G. L. *Handbook of Photochemistry*, 2nd ed.; Marcel Dekker: New York, 1993.
(46) Herzberg, G. *Molecular Spectra and Molecular Structure: Spectra of Diatomic Molecules*, 2nd ed.; Van Nostrand Reinhold: New York, 1950; Vol. 1.
(47) Schweitzer, C.; Mehrdad, Z.; Shafii, F.; Schmidt, R. *J. Phys. Chem. A* **2001**, *105*, 5309–5316.
(48) Rosenthal, S. J.; Xie, X.; Du, M.; Fleming, G. R. *J. Chem. Phys.* **1991**, *95*, 4715–4718.
(49) In recording absorption spectra, a MN-free, air-saturated sample of either ACN or CHX was used as the reference. Therefore, for MN-containing solutions, the only way to account properly for an MN-dependent change in refractive index, and hence an MN-dependent change in the extent of scattered light, is to take the difference between the O_2- and N_2-saturated MN-containing solutions.
(50) In air-saturated solutions at 760 Torr, $[O_2]_{ACN} = 1.9$ mM and $[O_2]_{CHX} = 2.4$ mM.[51] To our knowledge, the solubility of oxygen in MN has not been investigated.
(51) *Oxygen and Ozone*; Battino, R., Ed.; IUPAC Solubility Data Series 7; Pergamon Press: Oxford, U.K., 1981.
(52) Chattopadhyay, S. K.; Kumar, C. V.; Das, P. K. *J. Photochem.* **1985**, *30*, 81–91.
(53) In principle, one could envision that a small fraction of the CT_{FC} state could also couple directly to the MN triplet state, but in this case, it can still be shown that the qualitative features of the coupling scheme presented in Figure 8 remain unaltered; see the Supporting Information.
(54) It is interesting to note that to account for their data, McGarvey et al.[30] indicate that the efficiencies of $O_2(a^1\Delta_g)$ production by this doubly-excited state channel must be 0.08 and 0.16 in CHX and ACN, respectively, numbers that are consistent with our own data assigned to $O_2(a^1\Delta_g)$ production from the CT_{SE} states (Figure 8).
(55) Keszthelyi, T.; Weldon, D.; Andersen, T. N.; Poulsen, T. D.; Mikkelsen, K. V.; Ogilby, P. R. *Photochem. Photobiol.* **1999**, *70*, 531–539.
(56) Schmidt, R.; Tanielian, C.; Dunsbach, R.; Wolff, C. *J. Photochem. Photobiol., A* **1994**, *79*, 11–17.
(57) Marti, C.; Jürgens, O.; Cuenca, O.; Casals, M.; Nonell, S. *J. Photochem. Photobiol., A* **1996**, *97*, 11–18.
(58) Scurlock, R. D.; Mártire, D. O.; Ogilby, P. R.; Taylor, V. L.; Clough, R. L. *Macromolecules* **1994**, *27*, 4787–4794.
(59) Scurlock, R. D.; Nonell, S.; Braslavsky, S. E.; Ogilby, P. R. *J. Phys. Chem.* **1995**, *99*, 3521–3526.
(60) Wilkinson, F.; Helman, W. P.; Ross, A. B. *J. Phys. Chem. Ref. Data* **1995**, *24*, 663–1021.

JP905728D